LOCOMOTION PERFORMANCE CHARACTERISATION AND SEALING TESTING OF THE NANOKHOD MICROROVER DRIVE UNITS

Moritz Gewehr [(1)], Andreas Schneider [(2)], Josef Dalcolmo [(2)], Sabine Klinkner [(1)]

(1) University of Stuttgart, Institute of Space Systems
Pfaffenwaldring 29, 70569 Stuttgart, Germany
gewehr@irs.uni-stuttgart.de, klinkner@irs.uni-stuttgart.de
(2) von Hoerner & Sulger GmbH (vH&S), Schloßplatz 8, 68723 Schwetzingen, Germany
schneider@vh-s.de, dalcolmo@vh-s.de

1. ABSTRACT

Mobility is a key capability for planetary robotics and future surface exploration of celestial bodies. Locomotion Systems are hereby required to withstand extreme constrains resulting from the (dusty) planetary environment as well as a wide-scaled load and performance range due to the rover-soil interaction and operation. Since 2015, the University of Stuttgart`s Institute of Space Systems (IRS) and the company von Hoerner & Sulger GmbH (vH&S) are focussing on various development aspects for a future application of the Nanokhod Microrover for versatile Lunar surface mission scenarios [1] [2], thus continuing previous development steps of the Nanokhod Microrover within ESA`s BepiColombo mission to Mercury (MRP) [3]. The redesign of the rover maintains the general configuration of the two independently driven tracked locomotion units and a 2-DoF tiltable Payload Instrumentation Cabin (see Fig. 1 and 2), but is also optimising the system towards an anticipated long-term operation of the rover on the Lunar surface, using state of the art technologies and COTS components wherever possible. For operation of the rover with a low system mass between 3.2 kg to 4.5 kg depending on the rover configuration, four similar actuators are implemented in the rovers Mobility Unit plus an additional actuator within the rovers Tether Unit subsystem [4].

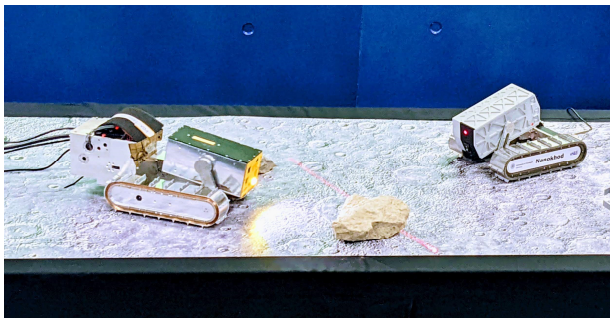

Figure 1: Nanokhod Microrover Breadboard Model

For the performance characterisation of the locomotion system and particularly the drive units of the rover, a modular test environment for several test scenarios was designed and operated within the space robotic lab at IRS. For the breadboard and laboratory models a low-fidelity test environment was set up. The test series described in this paper are categorised in three major disciplines: variable load, rpm and power characterisation on subsystem (single drive unit) level (1), sealing and abrasion testing within in a dust environment using the Lunar regolith simulant LHS-1 by Exolith [5] for excessive dust contamination testing (2) as well as a discussion of a Locomotion Unit performance testing and the setup of a Drawbar-Pull test environment for future full rover system performance characterisation. (3)

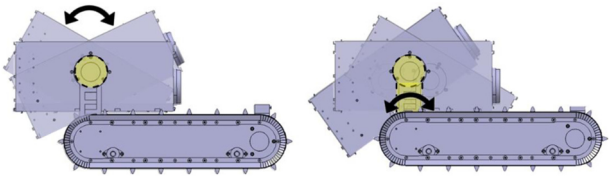

Figure 2: Nanokhod operational concept visualizing a 2-DoF movement of the central Payload Cabin located in between the two independently driven track-drive Locomotion Units of the Mobility Unit

2. NANOKHOD DRIVE UNIT DESIGN

As a key subsystem for the Nanokhod Microrover's mobile capabilities, the Drive Units were developed as highly integrated systems under challenging restrictions of severe environmental conditions, extreme miniaturisation and low power consumption but also high load performance requirements. Due to the tracked configuration of the rover - which is key for robust tractive capabilities of a micro rover system on a regolith surface - and an increase of mechanical complexity, respectively high load requirements for the drive units are required. For the development of the new drive units, four major requirement categories were defined as mandatory: highest possible degree of miniaturisation to fit in track width of 30 mm (1), low power consumption in order to be consistent with the rover power budget and

peak power consumption of max. 6 W (2), high load requirements of ~3.2 Nm in order to provide positive margins as well as handling and positioning of the rover's central payload instrumentation cabin (3), dust mitigation and sealing solution against regolith particles on the output shafts to prevent excessive contamination of critical components for a long term operation (4). As experienced in previous development stages, a modular integration of the drive units and optimised motor mounting was a desired design constraint in order to optimise the challenging integration process of the highly miniaturised components.

Figure 3: Development and integration of the new type of sealed high-performance micro Drive Units.

A new structure design allows both, a secondary sealing stage and an effective modular integration within the highly integrated locomotion units (Fig. 3). The total four Drive Units of the rover (two Track Drive Units, one Lever Drive Unit, one Payload Drive Unit) feature a similar design consisting of a brushless DC (BLDC) actuator with an actuator-sided gear head, a double-staged spur gear reduction stage, and a HFUC 8-100 Harmonic Drive gear. The output shafts of the Harmonic Drive gear are mounted to either the track wheel (Track Drive Unit) or the lever (Lever and Payload Drive Unit) connecting the rovers Mobility Unit with the Payload Cabin. Bearings are realised as small size dry-operated ceramic-hybrid bearings. In between Drive Unit internal and external moving parts spring enforced micro lid sealings are implemented, which shall prevent contamination of inlying components. Current design studies investigate two different brushless DC actuator solutions, which can both be mounted to a similar sealed gear-stage interface. The Enhanced Micro (EM) version is the smallest configuration with an enclosed volume of 69 mm by 30 mm. A follow up Advanced Mobility (AM) version of the Drive Units is currently being developed, which feature significant margins in torque and operational speed (see Tab. 1). As a baseline, the Drive Unit discussed in this paper is featuring the EM version of the rover. Within this study, a series of initial performance tests was elaborated, analysing the commanded and actual motor rotational speeds, the actuator current requirements and the respective output revolutions of the Drive Units. For both, the Track and the Lever Drive Unit a small sized test bench was set up in order to allow performance data characterisation the way these Drive Units are operated inside of the rover.

Table 1: Nanokhod Drive Unit Performance Characteristics

	BLDC Actuator & Gear Head	Spur Gear Transmission	Harmonic Drive HFUC-8-100	Track Wheel Output
Ratio	1 : 12	1 : 4.68	1 : 100	-
Efficiency	0.59	0.85	0.5	-
Velocity (nominal)	667 rpm[(1)] 44.6 rpm[(2)]	142 rpm[(1)] 9.54 rpm[(2)]	1,42 rpm[(1)] 0.095 rpm[(2)]	13,42 m/h[(1)] 0.899 m/h[(2)]
Torque (nominal)	28.88 mNm[(1)] 19.8 mNm[(2)]	114.91 mNm[(1)] 78.76 mNm[(2)]	5745 mNm[(1)] 3938 mNm[(2)]	5745 mNm[(1)] 3938 mNm[(2)]

[(1)] NK-AM: Nanokhod Advanced Mobility Version (nominal configuration)
[(2)] NK-EM: Nanokhod Enhanced Micro Version (smallest configuration)

To simulate worst case performance, the spur gear stages were dry operated. For the Harmonic Drive gears, a factory-sided minimum quantity lubrication is maintained in order to reduce wear damage. The test campaign aimed for deeper insight on the hardware performance aspects of the highly integrated drive units in order to consolidate design solutions for future development phases.

3. TRACK DRIVE UNIT PERFORMANCE TESTING

For the performance characterisation of the Track Drive Units of the rover, a test bench was developed allowing operation of the Drive Units as integrated within the final Locomotion Unit (see Fig. 4). The actuators are operated via the rover's locomotion controller, a small sized interface PCB operating the motor controllers and providing telemetry data to the rover's central core controller. Relevant telemetry data for the test series are the respective motor currents, controller sided in- and output velocities, voltage levels as well as the MCU temperature. During testing, a torque clutch is connected to the Drive Units output shaft connected to the track

wheel. A high resolution magnetic rotary encoder is directly attached to the output shaft, measuring the absolute angular position and output turning speeds. The encoder by RLS Renishaw provides an angular resolution of 131071 increments (0.0027466°) and data is received and recorded at 16 Hz. Via a spur gear transmission stage, the torque clutch is connected to an adjustable permanent magnetic hysteresis brake acting as a variable load. The break is mounted to a high-resolution torque sensor that allows measurement of the reaction moment on the load. The hysteresis brake by Mobac allows adjustable resistive torque from 0.001 Nm (0 % load) to 0.14 Nm (100 % load) at maximum continuous power dissipation of maximum 13 W.

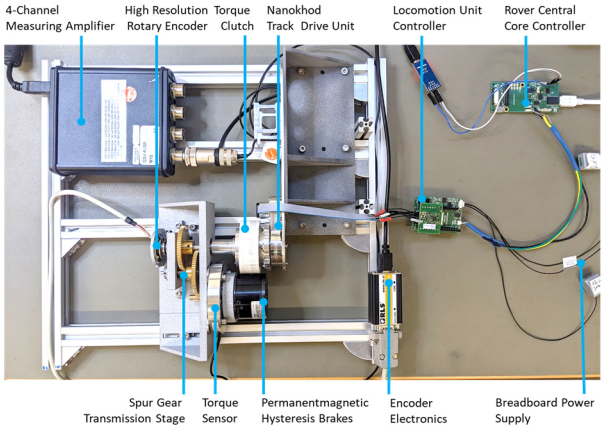

Figure 4: Drive Unit Performance Characterisation Test Bench

The torque sensor data is recorded at 12 Hz via a 4-channel measuring amplifier at the lab PC. Several load profiles were defined and tested in order to characterise the actuator performance, drive unit characteristics and efficiencies as well as the impact of the test bench on the performance data for calibration. For reliable and comparable data analyses characteristic output speeds at 1000, 3000 and 5000 rpm were defined as a nominal low to high performance spectrum. For an initial test series presented in this paper, eight calibration tests and four load tests were performed, defined by the hysteresis brake load level in between 0 %, 12.5 %, 25 %, and 37.5 %. For each load case, the defined motor speeds were tested at a continuous test time of 30 min each. Prior to the load tests, a calibration test of the test bench was performed, measuring the resistive torque within the gear and bearing assembly, as well as efficiency margins resulting from shaft offsets or misalignment. For the calibration test, an actuator was directly mounted on the torque sensor, and the averaged reaction torque for continuous rotation with and without the spur gear connected to the full test bench was measured. The calibration test showed a total (mechanical) efficiency of 83.959 % of the test bench setup. In combination with the spur gear stage setup a theoretical respective torque load between 0.064 Nm to 6.003 Nm can be applied to the Drive Units output shaft using the hysteresis brake. Fig. 5 shows a combined data set visualising the drive unit performance (motor current and controlled output revolutions) for idle load (0 %) and 25 % load at the three respective speed configurations of 1000 rpm, 3000 rpm, and 5000 rpm.

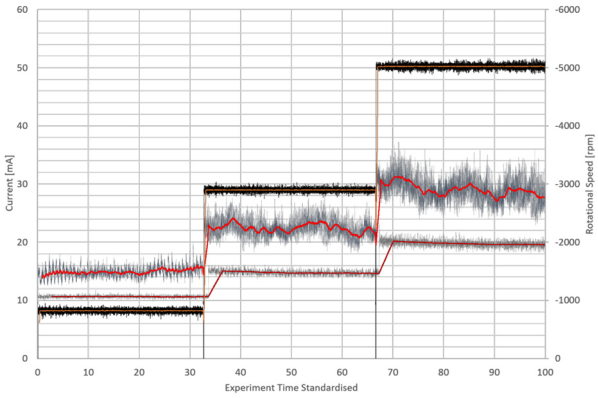

Figure 5: Track Drive Unit performance analysis visualized for two exemplary externally applied loads (0 % load in light gray/dark red averaged, 25 % load at dark gray/bright red averaged) at varying motor rotational speeds (black)

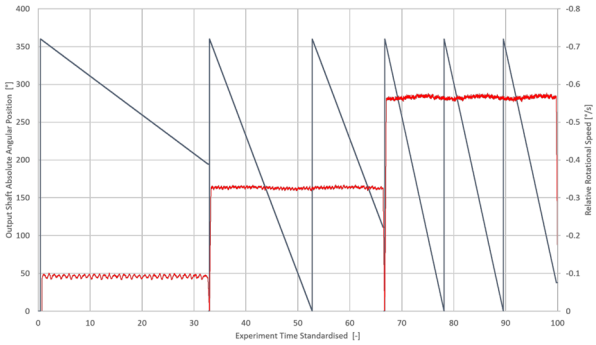

Figure 6: Monitored Drive Unit output shaft absolute angular position (dark gray) and relative rotational output speed (red) for 1000, 3000 and 5000 rpm input speed at 25 % load

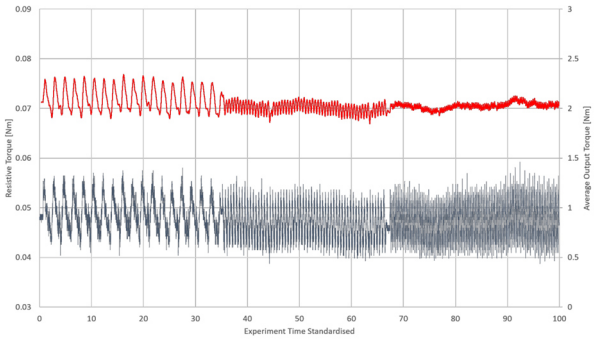

Figure 7: Measured torque sensor resistive torque of hysteresis brake (dark gray) and calculated resulting average torque at Track Drive Unit output shaft (red) for a respective 25 % load measurement.

In Fig. 6 the respective output shaft positions, and in Fig. 7 the torque sensor data for the 25 % load test are shown. It could be seen, that the hysteresis brake provides an alternating torque profile, especially during low rotational speeds, which results from the functional principle of the hysteresis brake. A more sensitive load (e.g. electrically controlled torque brake) could bring fewer alternating results. As the break is only mechanically adjusted by a coarse and nonlinear scale, a slightly variation in the set resistive load torque of the brake results in way higher output torques on the Drive Units output shaft. In this test, the 25 % load characteristic of the brake outperformed the resulting analytical 1,56 Nm by far, ending up with an average output torque of 2.04 Nm. Due to the torque sensor, these deviations can easily be detected, but the load scale might be misleading. Analysing the performance of the actuator, the Drive Units provide a significant high torque margin operating at only around 26.9 % of the tolerable continuous motor current during the measured peak currents in this test series.

4. LEVER DRIVE UNIT PERFORMANCE TESTING

As the Lever Drive Unit`s load characteristic is defined by operating the Payload Cabin as a point mass at the end of the lever, a respective single point mass test bench was set up. A model mass lever with exchangeable weights is attached to the Lever Drive Units output shaft in order to simulate the mass of moving a Payload Cabin (see Fig. 8).

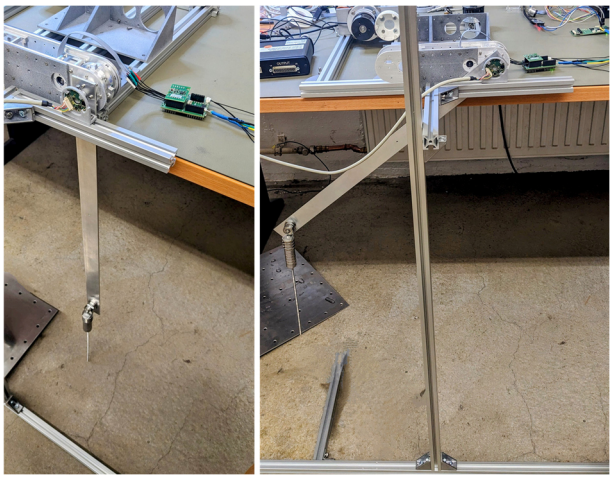

Figure 8: Lever Drive Unit torque load testing with a substitute lever and exchangeable point-mass weights.

Prior to testing, actuator and drive unit calibration measurements are performed, recording the actuator current and output shaft speed at characteristic 3000 rpm and 5000 rpm motor rotational speed. 1000 rpm were neglected as one full rotation of the lever would exceed reasonable experiment times. For performance testing within the initial test campaign two model loads were defined as a respective load mass of 1 kg and a doubled mass of 2 kg. For the chosen loads, a maximum resistive Lever Drive Unit output shaft torque under Earth gravity results in 0.6571 Nm and 1.3026 Nm respectively. For the initial test campaign, each experiment duration is set to 80 minutes, so that at least two full output rotations can be achieved at the lowest actuator rotational speed. Prior to testing, microscopic imaging was performed in order to analyse integrity of the drive units gear components. Data analysis visualised the cyclic load of the point mass with peak loads if the lever arm is in a respective horizontal position (see Fig. 9), thus acting the highest gravitational force on the lever. Performance analyses showed a consistent low motor current increase within the different test scenarios (17.050 mA for 1 kg mass, 17.431 mA for 2 kg mass at 3000 rpm, 23.818 mA for 1 kg mass and 24.731 mA for 2 kg mass at 5000 rpm). Table 2 shows the average and peak output of the test series, consisting of four major tests: actuator only, no load at 3000 rpm and 5000 rpm (#1), Lever Drive Unit mounted actuator, no load at 3000 rpm and 5000 rpm (#2), Lever Drive Unit with respective 1 kg load at 3000 rpm and 5000 rpm (#3), Lever Drive Unit with respective 2 kg load at 3000 rpm and 5000 rpm (#4).

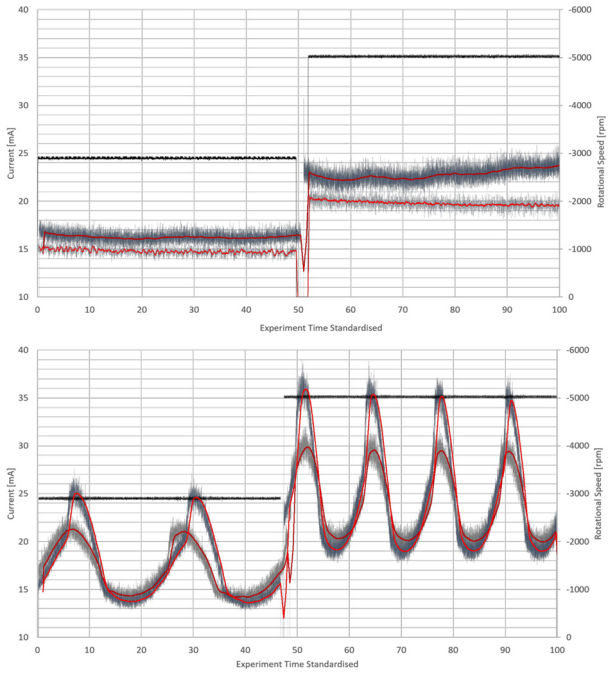

Figure 9: Lever Drive Unit performance telemetry: no-load tests (top) showing single actuator (light gray) and Drive Unit mounted (dark gray) testing at 3000 and 5000 rpm (black) and respective 1 kg (light gray) and 2 kg (dark gray) load testing (bottom) at equal motor rpm (black)

Table 2: Lever Drive Unit performance telemetry data analysed for each test scenario (actuator calibration (#1), Drive Unit no load (#2) and respective 1 kg (#3) and 2 kg (#4) load

CMD:	-3000.00 rpm					
Test	RPM AVG	Offset	Current AVG	Perc. Inc.	Current Peak	Perc. Inc.
#1	-2897.78 rpm	3.53 %	14.776 mA	-	16.211 mA	-
#2	-2898.00 rpm	3.52 %	16.256 mA	10.02 %	18.164 mA	12.05 %
#3	-2897.92 rpm	3.52 %	17.050 mA	4.88 %	23.926 mA	31.72 %
#4	-2897.94 rpm	3.52 %	17.431 mA	2.24 %	27.637 mA	15.51 %
CMD:	-5000.00 rpm					
Test	RPM AVG	Offset	Current AVG	Perc. Inc.	Current Peak	Perc. Inc.
#1	-5022.11 rpm	0.44 %	19.777 mA	-	22.852 mA	-
#2	-5022.28 rpm	0.45 %	22.803 mA	15.30 %	25.879 mA	13.25 %
#3	-5022.34 rpm	0.45 %	23.818 mA	4.45 %	32.129 mA	24.15 %
#4	-5022.47 rpm	0.45 %	24.731 mA	3.83 %	38.965 mA	21.28 %

As for the Track Drive Unit experiments, also for this test, analyses of the results demonstrate the high potential of the Drive Units, operating only at around 26.5 % of the tolerable continuous motor current during the measured peak currents in the test series (ambient laboratory environment conditions). A high-resolution encoder was mounted on an 3D printed adapter shaft on the output of the Lever Drive Unit in order to monitor the absolute position and relative output speed of the Drive Unit. Due to the necessary air gap between the torque lever and the encoder magnet and sensor read head in order to allow continuous 360° rotation of the lever, the highly sensitive encoder data showed a cyclic occurring series of bit error reasoned due to minimal positioning misalignments.

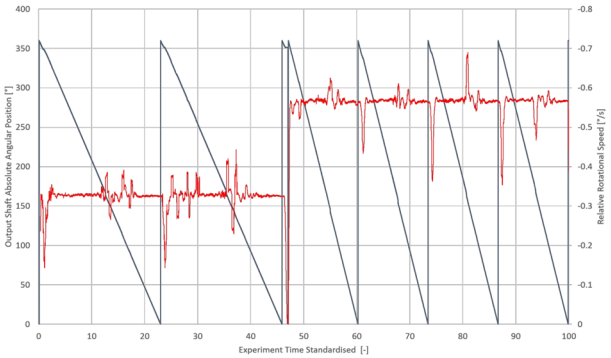

Figure 10: Encoder readout data showing the absolute position (dark gray) of the Lever Drive Unit output shaft and the relative rotational speed in degree per second (red).

Analysis of the data showed inconsistent data values when the bit error occurred, resulting in strong negative or positive data peaks (see Fig. 10). The inaccuracies are considered to be neglectable as no performance impact to the drive units from this additional sensor data set is induced. Follow-up studies will consider a high precision milled shaft adapter for accurate positioning on the encoder magnet to sensor head distance. The measured average relative output shaft rotation speed from the encoder data is -0.32377 °/s (3000 rpm input) and -0.56248 °/s (5000 rpm input) which fits the analytical calculated output speed with the measured actuator input speed by consistent 1.242 % (3000 rpm input) and 1.249 % (5000 rpm input) error. During post microscopic imaging minor abrasion effects were detected at the transmission spur gear stage (see Fig. 11), which could have resulted in the accumulation of small quantities of brass material in the bearing surface area. It is to be mentioned that the spur gear material pairing and specifically the lubrication selection of the Drive Units breadboard model within this study are not representative to a later development stage, which could reason the detected increased wear. Special start-up inflow phases or running up period of the drive unit could be considered depending on the long-term wear characteristics of the spur gears. Although the effects are quite modest, this will be further investigated in a follow-up design study.

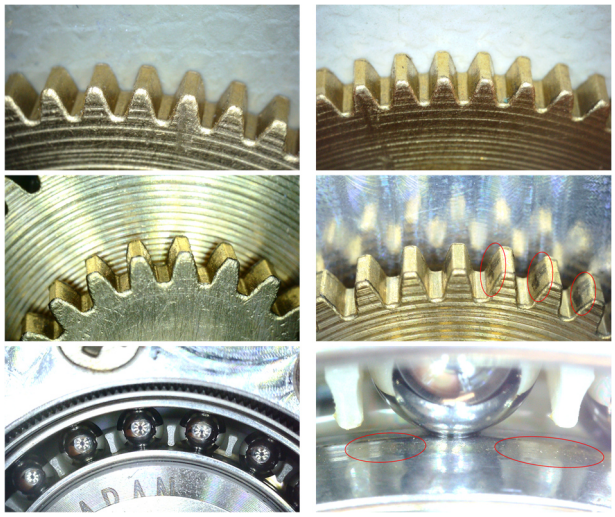

Figure 11: Microscopic imaging prior (left side) and post (right side) testing of wave generator spur gear (1st row), transmission stage spur gear (2nd row) and wave generator bearings (3rd row), detection of minor abrasion effects and small quantities of brass particles on the inner bearing surface marked

5. DUST CONTAMINATION AND SEALING TESTING

In order to characterise effects of severe interaction with dust particles and especially effects on the sealings, the Drive Units were operated in a dust environment using LHS-1 by Exolith [5] as a respective Lunar dust simulant. The simulant available could be seen as a sufficient representation of the particle grain size distribution in order to analyse the sealing performance. The Drive Units were mounted inside a low-fidelity dust test environment and covered with simulant particles.

Figure 12: Drive Unit Regolith Sealing Testing (top), gear stages under Microscopic Imaging (Harmonic Drive / bottom left, spur gear stage / bottom right)

As the Locomotion Units of the Nanokhod Microrover provide a robust first-stage primary sealing along the tracks, the degree of dust contamination simulated in this test exceeds an expected contamination level of the Drive Units by far. Nevertheless, the tests should analyse the performance under these excessive conditions, which could be relevant for long term applications. The test setup is shown in Fig. 12. In the initial test series, the Drive Units were operated for 90 minutes continuously while the actuator telemetry is being recorded. After the test, the Drive Units were completely cleaned and disintegrated for microscopic inspection. For the test, a consistent 5000 rpm actuator speed was defined to simulate the highest performance and in order to receive a highest number of output shaft revolutions throughout the test series. As shown in Fig. 13 the mean average actuator current consumption increased by roughly 14 % compared to a no-load idle operation, which is considered to result from the effort of moving significant amount of soil during the test as well as the higher friction in between the track wheel sealings and the Drive Unit structure.

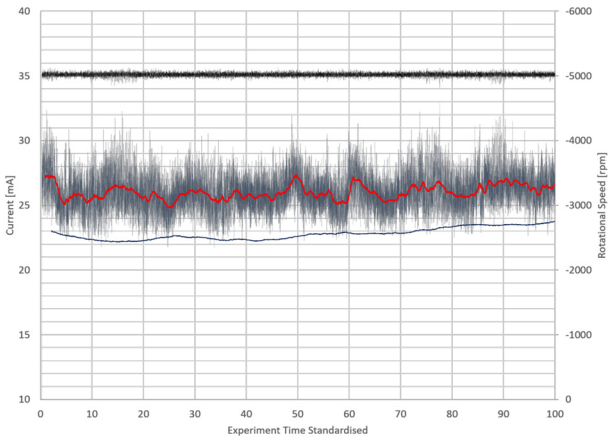

Figure 13: Actuator telemetry data showing the recorded motor current (gray) and averaged (red), a no-load comparison (dark-blue) and the actual motor rotational speed (black)

During the experiment, dust accumulated in the narrow space between the moving track wheel and the Drive Unit structure, which could also increase the load for the actuators. Despite the higher torque effort, the actuator showed no divergence in maintaining the demand speed of 5000 rpm.

Table 3: Recorded actuator performance data during dust contamination testing

	Current AVG	Current Peak	RPM AVG
No Load Test	22.803 mA	25.879 mA	-5021.94 rpm
Dust Sealing Test	26.014 mA	32.910 mA	-5021.70 rpm
Perc. Incr.	14.079 %	27.17 %	-0.00483 %

Step by step cleaning and disintegration of the Drive Units was handled carefully using soft Nylon brushes, small doses of Ethanol solution and cleaning wipes, in order not deteriorate the highly contaminated Drive Units. Nylon brushes showed a promising low surface abrasion in a previous study on Lunar dust mitigation methods and experiments at IRS [6] and were therefore also chosen for postprocessing of the dust contamination experiments. Contamination of the gap between the moving track wheel and the structure was severe as expected (see Fig 14). During cleaning also scratch marks of the particle abrasion effects were seen (right in Fig. 14). Further investigation will analyse if scratch marks could also result in a more representative dust contamination testing, and how severe the damage could propagate in long-term endurance tests.

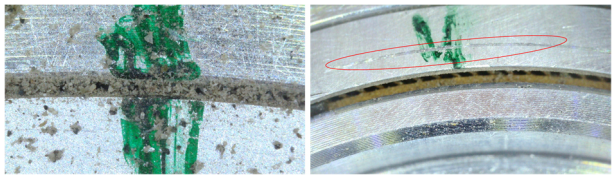

Figure 14: Severe dust contamination between track wheel and Drive Unit structure (left), visible scratch mark on track wheel at control point II (right)

After complete cleaning of the outer structure the sealed Drive Units were opened, and no dust particle contamination at the sensitive Harmonic Drive gear stage and the spur gears (2 and 3 in Fig 15) were detected. Also, no visible particles at the inlying track wheel structure (4 in Fig. 15) could be seen. Although the test times were short, at this severe level of initial dust contamination the primary sealing of the Drive Units showed good results. In a last step, the track wheel and spring-enforced lid sealing were disassembled. Comparison to microscopic imaging prior to the test (1-1) after disassembly (1-2) and after cleaning of the sealing lid (1-3) showed no damage to the sealing material (Fig. 15). The dust contamination tests showed promising results for the first breadboard

model of the Drive Units sealing performance, but further testing is highly recommended. This should include long term endurance testing, and also respect thermal variation in later stages.

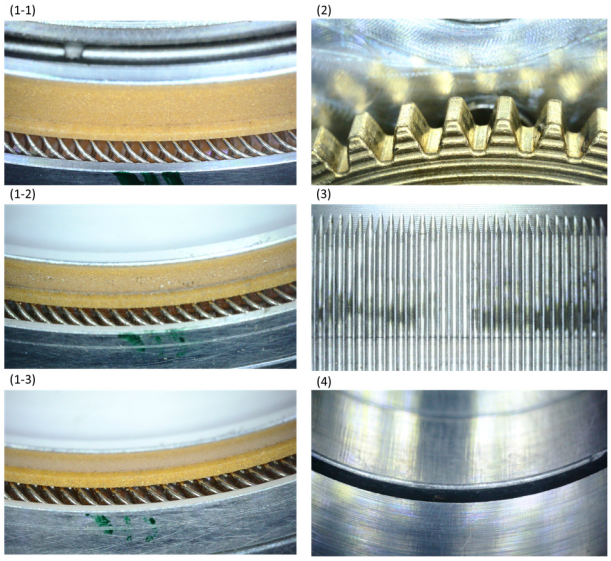

Figure 15: Microscopic imaging of the primary spring enforced lid sealing at control point III before testing (1-1), after disintegration (1-2) and after cleaning (1-3) showing no damage to the sealing material, inspection of the spur gear (2), Harmonic Drive Flexspline (3) and inlying Aluminium structure (4) after testing showing no visible presence of dust particles.

6. LOCOMOTION UNIT TEST ENVIRONMENT

For full Locomotion Unit tests, ongoing development activities focus on the setup of a modular test environment allowing both: single track performance testing, and a full rover performance testing and characterisation of respective performance parameters like the Drawbar Pull and sinkage into various soil substrates. The initial setup of the test bench features a torque-sensor coupled high-performance brushless DC actuator and planetary gearhead, which allows via a belt-drive transmission stage a controlled deployment of a steel wire cable, thus simulating the Drawbar Pull (see Fig. 16). The full transmission stage allows resistive forces of over 300 N, and is intended to be also used for various other robotic applications of the IRS space robotics laboratory. Within the developed modular Drawbar Pull test environment either the full rover can be connected to the steel wire or a single Locomotion Unit drawbar-sledge can be used. The low-friction and passive 2-DoF lever sledge can apply various respective vertical loads on the Locomotion Unit by mounting of counter weights, simulating individual load cases or gravitational impacts (see Fig. 16). For performance analyses the induced centre of mass can also be configured in order to simulate a shift of CoG due to operation of the Nanokhod Microrover's central Payload Cabin. The sledge is connected via an additional axial force sensor to the steel wire in order to allow controlled Drawbar Pull measurements. In between the interface to the Locomotion Unit, a torque sensor allows detection of torsion forces exerted by operation of the single Locomotion Unit on the variable soil underneath. Initial calibration tests showed an induced 3,70 N vertical load of the sledge lever in a nominal configuration. For initial tests, counter weights were selected to induce a weight load of ~15,55 N, simulating roughly half of the Nanokhod rover weight in a central CoG configuration under Earth gravity.

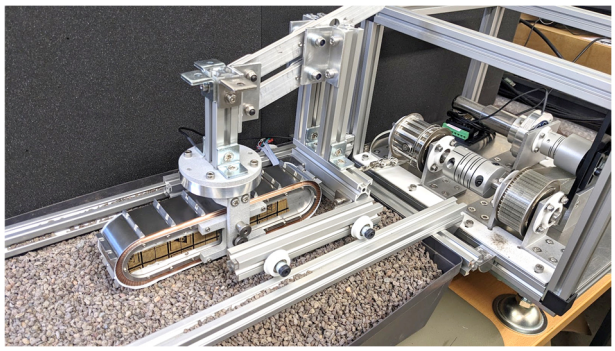

Figure 16: IRS Drawbar Pull Performance Test Environment for single Locomotion Unit testing with a low friction sledge simulating variable weight loads.

Prior to full Drawbar Pull testing, within an initial test series, the modular drive units were fully integrated into the Locomotion Units including the circumferential enclosed primary spring sealing and mounted into a zero-load configuration (see Fig. 17), allowing to characterise the internal friction of the mechanical track drive setup at a no-load characteristic. An average Track Drive Unit power consumption of ~ 0.41 W at 5000 rpm was measured in a 30 min dry run, resulting in a first preliminary measured (mechanical) efficiency of ~ 47.595 %. Further testing is required for a consistent validation of these parameters.

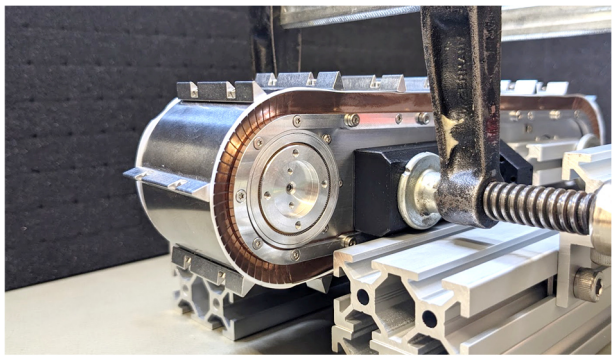

Figure 17: Fully integrated Locomotion Unit in a zero-load configuration

Follow-up single Locomotion Unit Drawbar-Pull performance tests on a small scaled loose basalt gravel test-bed as shown in Fig. 16 achieved a DP performance of ~13.20 N before the test was aborted due to excessive slippage. An exemplary data set is shown in Fig. 18, visualizing the Drawbar Pull force measured by the axial force sensors (blue), the slight increase of the Track Drive Unit actuator currents (light gray) and the no-load single Track Drive Unit calibration actuator current (dark gray) as a comparison.

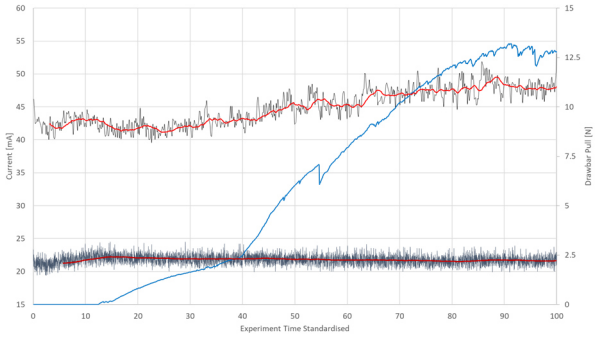

Figure 18: Actuator telemetry data during single Locomotion Unit Drawbar-Pull testing on an exemplary loose basalt grain soil bed and recorded Drawbar-Pull force from the axial force sensor (blue)

The implementation of the Drawbar Pull performance test bench to a controlled Lunar Simulant testbed with respective known soil parameters is part of ongoing research activities, increasing the performance characterisation data set significantly. Exemplary as a modular interface, the Drawbar Pull test bench assembly can be integrated to the Lunar Dust Simulant Environment (as shown in Fig. 19), or even placed into larger soil beds up to open field tests. Ongoing activities also include the in-depth validation of the performance and test data with developed analytical as well as simulation-based assessments for light-weight and small scaled tracked locomotion applications, as hereby especially large variations to classical wheel-soil interaction models need to be respected.

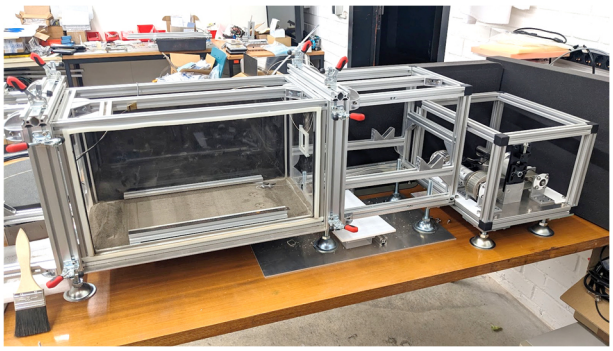

Figure 19: Drawbar Pull Test bench attached to a small-scaled Lunar Simulant Dust soil bed environment within the IRS laboratories

SUMMARY

Within this paper a performance characterisation for the Nanokhod Microrover Drive Units within an initial test series is discussed. The Drive Units were undertaken several load tests representative for a future application. As operated under Earth gravity, the load requirements are exceeding required torque performance for an operation under Lunar gravity by far, thus providing valuable margins in performance of the rover, thus also reasoning current investigations of a scalability option of the rover system. The paper describes ongoing activities for in-depth characterisation of the mobile capabilities of the rover system and valuable developments steps to increase its technological readiness for a future application.

REFERENCES

[1] M. Gewehr, A. Schneider, J. Dalcolmo, S. Klinkner, *Mission Concepts and New Technologies for Lunar Surface Exploration using the Nanokhod Microrover*, Proceedings of 73rd International Astronautical Congress (IAC), Paris, France, 2022

[2] M. Nitz, A. Schneider, J. Dalcolmo, S. Klinkner, *Design and Testing of a Novel Miniaturised Sealed Tether-Recoil Mechanism for the Nanokhod Rover,* 19th European Space Mechanisms and Tribology Symposium (ESMATS), online, 2021

[3] C.G. Lee, S. Klinkner, W. Hlawatsch, et al. *Mercury Nanokhod Rover – Hardware Realisation and Testing*, ASTRA 2006, Noordwijk, The Netherlands, 2006

[4] M. Gewehr, A. Schneider, J. Dalcolmo, S. Klinkner, *The Nanokhod Microrover – Using State Of The Art Technology For Accessing Pristine Sites Of Scientific Interest On The Moon*, Proceedings of ESA ASTRA 2022 Conference, ESTEC Noordwijk, The Netherlands, 2022

[5] Exolith Lab, *LMS-1 & LHS-1 Lunar Simulant Fact Sheet & SDS*. University of Florida, Orlando, USA, 2019

[6] M. Gewehr, A. Al-Barwani, D. Bölke, S. Klinkner, *Assessment of Methods and Strategies for Lunar Dust Mitigation Experiments within a Low-Fidelity Test Environment*. Proceedings of DLRK Conference 2023, Stuttgart, Germany, 2023